PAPER • **OPEN ACCESS**

Investigation of the gamma ray shielding properties of Epoxy based on Bi_2O_3/GO nanocomposite

To cite this article: Waleed F. Khalil *et al* 2024 *J. Phys.: Conf. Ser.* **2830** 012023

Journal of Physics: Conference Series **2830** (2024) 012023 doi:10.1088/1742-6596/2830/1/012023

Investigation of the gamma ray shielding properties of Epoxy based on Bi_2O_3/GO nanocomposite

Waleed F. Khalil[1], Fawzia Mubarak[1], Ahmed Agha[1], R. S. Zaky[1], Fatma A. Kamel[2]

[1] Nuclear and Radiological Safety Research Centre (NRSRC), Egyptian Atomic Energy Authority (EAEA).
[2] Material Science and Nanotechnology Department, Faculty of Postgraduate Studies for Advanced Sciences (PSAS) Beni-Suef University, 62511 Beni-Suef, Egypt

waleed_fekry12878@yahoo.com

Abstract. One of the important carbon materials, graphene oxide (GO), has several oxygen-containing functional groups. Due to its unique structure, it has attracted increasing interest in multidisciplinary studies of physical and chemical attributes. In this work, Bismuth Oxide nanoparticles (Bi_2O_3) is prepared and functionalized with graphene oxide nanosheets (Bi_2O_3-GO). The Bi_2O_3 and Bi_2O_3-GO nanocomposite were mixed with epoxy by changing the percentages to 1%, 2.5%, 5%, and 10%. The study used a hyper-pure germanium detector to investigate the attenuation characteristics of the prepared samples. Ba^{133}, Cs^{137}, and Co^{60} point sources were used at photon energies of 81, 276, 302, 356, and 383 keV for Ba^{133}, 661 keV for Cs^{137}, and 1173 and 1332 keV for Co^{60}. The linear attenuation coefficient, mass attenuation coefficient, half-value layer, and tenth-value layer were estimated to investigate the radiation shielding characteristics of the prepared samples. The linear attenuation coefficient (μ) values varied from 0.45 to 0.88, 0.23 to 0.89, and 0.31 to 0.77 for Ba^{133}, Cs^{137}, and Co^{60}, respectively. The mass attenuation coefficient (μm) values varied from 0.18 to 0.50, 0.19 to 0.50, and 0.15 to 0.50 for Ba^{133}, Cs^{137}, and Co^{60}, respectively. Half-value layer (HVL) values varied from 0.79 to 1.55, 0.78 to 3.07, and 0.9 to 2.26 for Ba^{133}, Cs^{137}, and Co^{60}, respectively. Tenth-value layer (TVL) values varied from 2.61 to 5.16, 2.58 to 10.19, and 2.98 to 7.51 for Ba^{133}, Cs^{137}, and Co^{60}, respectively.

Keywords: Bi_2O_3; Graphene Oxide; Epoxy; Gamma Ray; Shielding properties.

1. Introduction

Today, radiation present everywhere, and applications of radioisotopes are growing in industry, agriculture, medicine, and many other fields and daily activities. Radiation has serious effects and impacts on man and the environment, so proper radiation shielding must be used for human safety and protection. The proper shielding made from natural or synthetic material. In this study, the material was synthesized on the basis of highest efficiency at the lowest cost. High density material like lead can attenuate a wide range of radiation types, despite its excellent protection, lead-based shielding is unpleasant to wear and heavy in weight. There is a desire for lightweight and comfortable radiation shielding that can protect the human body from radiation's harmful effects. Polymeric materials are suitable for wearable clothes since they are lightweight and comfortable. However, polymers do not provide significant radiation-shielding

properties on their own. Polymers are reinforced with non-toxic heavy element that have high radiation absorption coefficients [1, 2]. Polymer-based carbon nanomaterials, when combined with inorganic nanoparticles (TiO_2, MoS_2, and $BaTiO_3$), improve the ability to absorb electromagnetic waves and also enhance mechanical and thermal stability [3]. The addition of GO increased the electrical conductivity and EMI shielding efficacy of the produced composites. At a frequency of 3 GHz, increasing GO to 1 php increased shielding efficacy by 17.35% and 16.94% at 0 and 200 kGy, respectively [4]. Graphene is an excellent EM absorber due to its broad interface, high dielectric loss, and low density. Pure graphene's conductive and electromagnetic properties are too high for the impedance matching standard, resulting in strong reflection and poor absorption.The specific integration of some metal oxide semiconductor crystals on rGO sheets allows for the construction of EM-absorbing metal oxide semiconductor/carbon hybrids. Fe2O3 formed on rGO has a unique microstructure, which explains its low EM reflection coefficient (RC) and wide effective absorption bandwidth [5]

2. Materials and method

The materials were used in this study as follows: Graphite powder with Potassium Permanganate ($KMnO_4$), Sulfuric Acid (H_2SO_4, 98%), Bismuth (III) Nitrate ($Bi(NO_3)_3$, Phosphoric Acid (H_3PO_4, 85%), Hydrogen Peroxide (H_2O_2, 30%), Nitric Acid (Sigma Aldrich,68%), Hydrochloric Acid (HCl, 36.5%), Ethanol, and Methanol (Sigma Aldrich,99%), Sodium Hydroxide (NaOH, Sigma Aldrich,99%) Epoxy Polymer (resin & hardener) all chemical were used without further purification and Ultra-pure water.

2.1 Preparation of graphene oxide

Graphene oxide was produced from graphite powder using an enhanced version of the Hummers' process, as described by Waleed F. Khalil et al. in 2022 [2], The steps below were taken to oxidize GO: a) In an ice path (with a temperature below 0 degrees Celsius), concentrated H_2SO_4 and H_3PO_4 (2:1) were used to strongly oxidize graphite while it was being stirred vigorously; this was followed by slowly adding $KMnO_4$ (18 g/3 g graphite) to the mixture that was already there. b) The oxidized GO suspension was poured on iced water containing H_2O_2 (30 wt%) and exfoliated in water by ultra-sonic wave. c) GO was washed several times by HCL 10 % and deionized water through centrifugation. d) The resultant GO was dried under vacuum at 60 °C.

2.2 Synthesis of Bi_2O_3Nano particles

In the hydrothermal synthesis method, a solution of 0.3M Nitric acid with a volume of 50 mL employed to dissolve 1 mmol of Bismuth (III) Nitrate Hexahydrate. The surface was eliminated by the application of an ultrasonic wave after the introduction of the oxidized GO solution into cold water containing 30% H_2O_2. A homogeneous mixture was achieved by sonicating the fluid for 15 minutes at room temperature. Next, a 0.2 M Sodium Hydroxide solution with 5–6 mmol (1:5 molar ratio of $Bi(NO_3)_3.5H_2O$ to NaOH) was gently added to the clear solution while stirring vigorously. The pH of the mixture progressively increased during the reaction, reaching roughly above 10, which initiated the precipitation process, resulting in the formation of a white precipitate. After centrifugation for 30 minutes, the white solid formed and transferred to an autoclave with a Teflon liner. After that, it underwent hydrothermal treatment, which entailed maintaining a temperature of 160 °C for twelve hours. Without any outside help, the autoclave was left to cool down to ambient temperature. After 6 minutes of centrifugation at 7500 rpm, the yellow precipitate created. In the next steps, it rinsed many times with ultra-pure water and dried for 12 hours at 80°C. Additional characterization carried out after the products were calcined at a temperature of 450 oC for three hours [6].

2.3 Preparation of GO- Bi_2O_3 Nano particles

To functionalize the surface of GO nanosheets with Bismuth Oxide, studies used the Abdolahzadeh et al. (2022) [7] approach with a modest modification. Specifically, 0.5 g of graphene oxide (GO) was added to 100 mL of Ethanol and revolved for 10 minutes at 50°C. The Ethanol/GO mixture was mixed with 2.5 grams of Bismuth Oxide in 250 mL of deionized water and reacted for 30 minutes at 60°C. Immediately, the round-bottom flask was filled with 40 mL of NH_3 and 10 mL of HCl. The suspension should agitate for 48 hours at a temperature of 80 °C. Once obtained, the additives referred to as GO-Bi_2O_3, were dried at a temperature of 80°C [7].

2.4 Preparation Epoxy/Bi_2O_3 and Epoxy/GO- Bi_2O_3

In this study, we synthesized epoxy resin composites with Bi_2O_3 and Bi_2O_3-GO for radiation shielding. To prepare the epoxy nanocomposite samples, we combined the epoxy resin with the hardener following the manufacturer's instructions, which provide a 1:1 ratio of 3 g of epoxy resin to 3 g of hardener. The pure Bi_2O_3 and Bi_2O_3-GO powders added in concentrations of 1%, 2.5%, 5%, and 10% by weight. For proper distribution of particles inside the matrix, vigorously swirl the liquid using magnetic stirring for 15 minutes. The well-combined material put onto a circular plastic petri dish measuring 6 cm diameter and left to dry overnight at 60 °C [1]. In the upcoming part, we will utilize the following codes for the produced samples: S1, S2, S3, S4, S5, S6, S7, S8 and S9 as shown in figure 3. Table 1 summarizes the composition of the newly generated 9 samples with different concentrations.

2.5 $Bi_2O_3$and epoxy/GO- Bi_2O_3examples characterized.

Using the ATR method (PerkinElmer, spectrum 2, USA), the FTIR spectra of epoxy, Bi_2O_3, and epoxy/GO- Bi_2O_3were characterized. The device is an X-ray diffractometer made by Shimadzu, with a Cu radiation wavelength of 1.54056 Å. Point sources of Ba133, Cs137, and Co60 had been used at photon energies of 81, 276, 302, 356, 383 keV, 661 keV, and 1173, 1332 keV, respectively, in a γ-ray spectrometer that utilized a high-purity germanium (HPGe) detector/ORTEC. The spectrometer energy calibration was performed. The present study used Transmission Electron Microscopy (TEM) with a JEOL-JEM 2100 instrument manufactured in Japan. The EVO-MA10 scanning electron microscope from ZEISS studied the surface morphology.

2.6 γ-ray attenuation parameters' evaluations

To investigate the attenuation characteristics of synthesized samples, gamma-rays were measured for different concentrations by using different photon energies of point sources: Ba133, Cs137, and Co60. 81, 276, 302, 356,383 keV lines were measured for Ba133. For Cs137, gamma energy of 661.6 keV was measured, and finally, 1173 and 1332 keV were measured for Co60. A hyper-pure germanium detector was used. The count rate for each energy was measured for the reference sample and then for each sample of different concentrations. The Following equations used to calculate the linear attenuation coefficient (μ), mass attenuation coefficient (μm), half-value layer (HVL),and tenth-value layer (TVL): The slope of the relation between relative intensity (I/Io) and sample thickness (X) used to obtain the linear attenuation coefficient (μ, cm-1) [8].

$$\mathbf{I = I_{0}e^{-\mu x}} \qquad \mathbf{(1)}$$

The gamma-ray intensity (I_o) without thicknesses and the sample intensity (I) defined as:

$$\mathbf{\frac{I}{I_o} = e^{-\mu x}} \qquad \mathbf{(2)}$$

Mass attenuation coefficient (μm, cm^2. g^{-1}) can be calculated from the linear attenuation coefficient (μ), as:

$$\mathbf{\mu m = \mu/\rho} \qquad \mathbf{(3)}$$

The density of the synthesized substance at various concentrations denoted by ρ. A half-value layer (HVL) a thickness that reduces the gamma radiation's intensity by half its value; calculation as follows:

$$\mathbf{HVL=Ln\ 2/\mu} \qquad \mathbf{(4)}$$

Where the thickness attenuates the intensity of gamma radiation tenth of its value called a tenth-value layer (TVL), and calculated as following:

$$\mathbf{TVL=ln\ 10/\mu} \qquad \mathbf{(5)}$$

3. Results and discussion

3.1 Characterization of GO, Epoxy $Bi_2O_3$and Epoxy/GO Bi_2O_3

Before and after oxidation, we performed XRD analysis to the graphite powder. A peak at 2 theta = 26.1695º, as seen in Figure 1a, indicates that the graphite powder has a d-spacing of 3.34 Å. Following oxidation, the graphite peak disappeared, and a graphene oxide peak appeared at 2-theta = 10.2°. The d-spacing value increased to 8.0427 Å by inserting function groups between graphite layers. A considerable amount of graphite oxidized during the creation of graphene oxide. The results obtained full in agreement with the previous research [9, 10]. Raman spectroscopy helps characterize GO as shown in figure 1b. The Raman spectroscopy of GO exhibits two significant D bands at 1343 cm^{-1} and a G-band at 1594 cm^{-1}. ID/IG was 0.9945 for D and G bands. These findings match earlier research [11, 12]. The HRTEM and SEM images of graphene oxide displayed in Figures c and d. A transparent, flat, and slightly wrinkled surface characterizes the graphene oxide-layered structure.

Figure 2 shows the FT-IR spectra for pure GO, epoxy, Bi_2O_3, and epoxy/GO Bi_2O_3-modified GO. The stretching vibrations of C-O, C-OH, C=O, C-C, COOH, and O-H bonds represented peaks at 1080, 1155, 1228, 1286, 1639, 1734, and 3431 cm^{-1} in the spectra of pure GO, which corresponds to various oxygen-containing functional groups. The presence of peaks corresponding to functional groups in both the spectra of GO and Bi_2O_3confirms the potential for molecular bonding between GO and Bi_2O_3. A peak around 500–700 cm^{-1} observed in both composites, indicating the telescopic vibration of the Bi-O bond in Bi_2O_3, and a peak at 849 cm^{-1} attributed to the Bi-O-Bi bond [13, 14].

Furthermore, at 3430 cm^{-1}, there is O-H stretching vibration of adsorbed water, and at 1455 cm^{-1}, there is O-H stretching vibration peak in C-O-H. The C=O bond in COOH is responsible for the antisymmetric stretching vibration at 1440 cm^{-1} and the symmetry stretching vibration at 1606 cm^{-1}. The carbons in oxirane ring associated with the 2966 cm^{-1} wavenumber peaks in the epoxide FTIR spectra, while the stretching vibration of CH_2 (aliphatic carbons) results in the 2921 cm^{-1} and 2859 cm^{-1}peaks. Moreover, carbonyl stretching vibration and CH_2 bending vibration associated with the peaks at 1745 cm^{-1} and 1455 cm^{-1}, respectively. Furthermore, peaks observed at 733 cm^{-1}, 1388 cm^{-1}, and 3429 cm^{-1} can be attributed to oscillatory vibration of CH_2 and bending and stretching vibrations of O-H bonds, respectively. The added presence of these functional groups can enhance the dispersion quality of GO- Bi_2O_3 inside the matrix [15-17].

3.2. Effect of mixing $Bi_2O_3$and GO- Bi_2O_3 with Epoxy for γ-ray shielding properties

In general, results show that, sample 4 improved the attenuation characteristics compared with the reference sample 1. While sample 8 and 9 show highest improvement compared to that of references samples 1,5 and 6. As shown in table (2) the linear attenuation coefficient for sample 4 increased from 0.45 to 0.50 at Ba133 line energy of 356 keV. For 661.6 keV energy line of Cs137, the linear attenuation coefficient increased from 0.23 to 0.64. While for 1332 keV it increased from 0.31 to 0.49. In other hand, sample 8 and 9 show increasing of linear attenuation coefficients from 0.5 to 0.87 and 0.88 respectively for Ba133 line energy of 356 keV. For 661.6 keV energy line of Cs137, the linear attenuation coefficient increased for samples 8 and 9 from 0.51 to 0.87 and 0.80 respectively. While for 1332 keV it increased from 0.40 to 0.76 and 0.77

for samples 8 and 9 respectively. Tables (1&2) and Figures (3&4) show the improvement of other attenuation parameters as mass attenuation coefficients, half value layers and Tenth value layers.

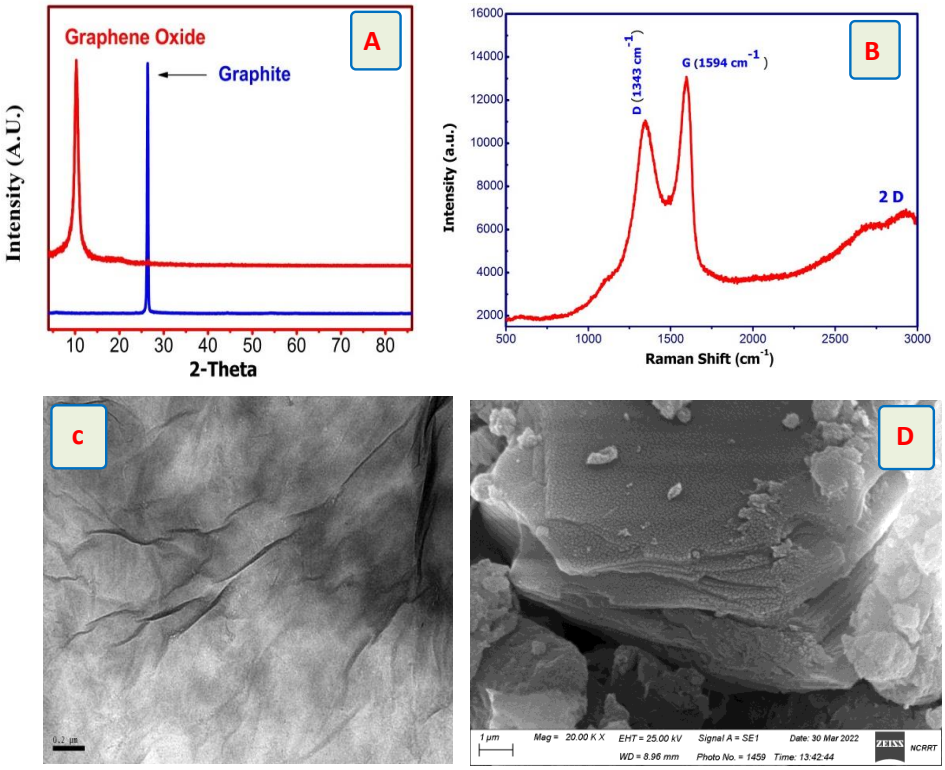

Figure 1. XRD patterns of GO and Graphite (a), Raman spectra of GO (b), HRTEM image of pure GO (c), and SEM image of GO- Bi_2O_3nanocomposite (d).

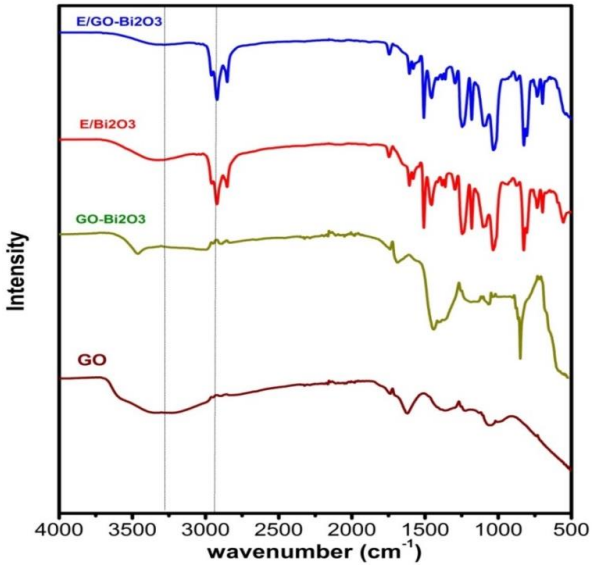

Figure 2. FTIR spectra of graphene oxide pure, GO- Bi_2O_3, epoxy- Bi_2O_3, and epoxy/GO- Bi_2O_3.

Table 1. The description and component content of the nanocomposites from Bi_2O_3 and GO.

code	Sample description	Percentage % of Bi_2O_3	Density g/cm^3
S1	Epoxy	0.0%	1.2
S2	Epoxy/ Bi_2O_3	1.0 %	2.4
S3	Epoxy / Bi_2O_3	2.5 %	2.5
S4	Epoxy / Bi_2O_3	5.0 %	2.8
S5	Epoxy / Bi_2O_3	10.0 %	2.5
S6	Epoxy Bi_2O_3–GO	1.0%	1.4
S7	Epoxy/ Bi_2O_3– GO	2.5%	1.5
S8	Epoxy/ Bi_2O_3–GO	5.0%	1.8
S9	Epoxy / Bi_2O_3–GO	10.0%	2.4

Attenuation coefficient is the quantity that characterizes how easily electromagnetic radiation penetrates a material. The linear attenuation coefficient (μ) is the probability of any type of interaction (PE, CS, PP) per unit path length, but it is hard to find, so a related quantity, the mass attenuation coefficient (μm), are easy to find. The mass attenuation coefficient is the linear attenuation divided by the density of the material (μ /ρ). It is the probability of an interaction (PE, CS, PP) per unit density thickness cm^2/g. The value of the mass attenuation coefficient depends on the shielding material and the energy of the photons. At low photon energies of gamma radiation attenuation is dominated by photoelectric absorption while at medium energies Compton scattering is the common process and at high energies pair production is the dominant one. Gamma attenuation coefficients are directly proportional to the atomic number of the element(s) from which the shielding material is constructed. So, table 2 shows that mass attenuation coefficients for samples 8 & 9 show good attenuation parameters due to its improved structure [18].

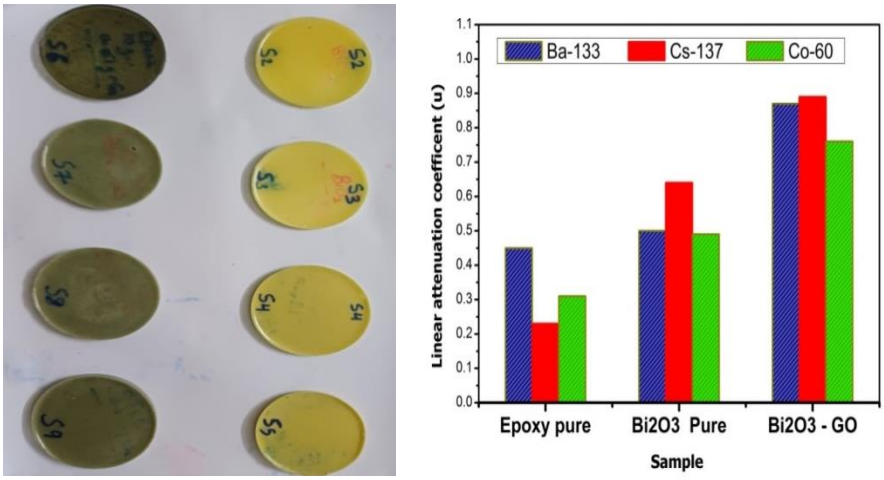

Figure 3. (a) A photograph of the synthesized samples for epoxy/ $Bi_2O_3$and epoxy/GO- $Bi_2O_3$with different concentrations and (b) is linear attenuation coefficient (μ, cm^{-1}).

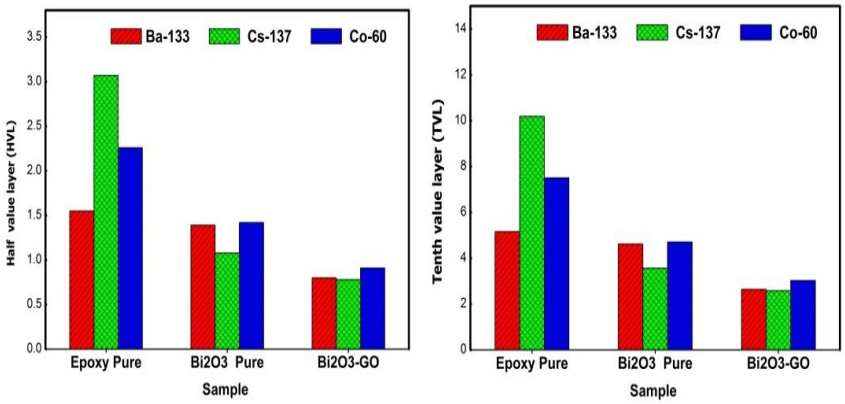

Figure 4. Half-value layer values and Tenth-value layer (TVL) for Epoxy, Epoxy/ Bi_2O_3, and Epoxy/GO- $Bi_2O_3$of Ba^{133}, Cs^{137}, and Co^{60} point sources.

Table (2), Mass Attenuation Coefficient (μm) of prepared sample at energy from 81 to 1332 (kev).

	Mass Attenuation Coefficient (μm)							
	Energy (kev)							
Sample	**81.00**	**276.00**	**302.00**	**356.00**	**383.00**	**661.60**	**1173.00**	**1332.00**
S1	0.69	1.34	1.07	0.37	0.98	0.19	0.19	0.26
S2	0.52	0.38	0.34	0.26	0.29	0.23	0.12	0.15
S3	0.14	0.01	0.22	0.24	0.23	0.22	0.16	0.15
S4	0.14	0.02	0.18	0.18	0.17	0.23	0.11	0.17
S5	0.22	0.10	0.25	0.22	0.26	0.26	0.14	0.16
S6	0.14	0.06	0.27	0.36	0.43	0.37	0.44	0.50
S7	0.35	0.28	0.47	0.50	0.59	0.49	0.32	0.41
S8	0.34	0.16	0.49	0.48	0.48	0.50	0.46	0.42
S9	0.28	0.25	0.37	0.37	0.47	0.34	0.29	0.32

4. Conclusion

In this study, slight modifications to the improved Hammer method used for producing graphene oxide (GO) have been used. The researchers modified a prepared graphene oxide with Bi2O3using a practical approach. $Bi_2O_3$and GO-Bi_2O_3 nanocomposites were added to the epoxy (1 to 10 wt%). Results show that GO-Bi_2O_3 nanocomposites effectively guard against γ-ray radiation. Adding more filler to composites enhances their ability to block γ-ray radiation by increasing radiopacity. Sample 8 and 9 improved the attenuation parameters at all photon energies as compared with sample 1, 5 and 6 compositions. It can be concluded that the composition of sample 8 and 9 have a good significant effectiveness on the attenuation parameters, and it is adequate and effective gamma radiation shielding.

References

[1] H. Hale Aygün, M. Hakkı Alma, ChemistrySelect, 7 (2022) e202202118.
[2] W.F. Khalil, A. Agha, R. Rayan, Journal of Physics: Conference Series, IOP Publishing, 2022, pp. 012014.
[3] L. Vovchenko, O. Lozitsky, L. Matzui, V. Oliynyk, V. Zagorodnii, M. Skoryk, Materials Chemistry and Physics, 240 (2020) 122234.
[4] E.H. Awad, K.F. El-Nemr, M. Atta, A. Abdel-Hakim, A. Sharaf, Radiation Physics and Chemistry, 203 (2023) 110629.

[5] L. Kong, X. Yin, Y. Zhang, X. Yuan, Q. Li, F. Ye, L. Cheng, L. Zhang, The Journal of Physical Chemistry C, 117 (2013) 19701-19711.
[6] R. Jha, R. Pasricha, V. Ravi, Ceramics international, 31 (2005) 495-497.
[7] T. Abdolahzadeh, J. Morshedian, S. Ahmadi, Polyolefins Journal, 9 (2022) 73-83.
[8] A. Shahboub, G. El Damrawi, A. Saleh, The European Physical Journal Plus, 136 (2021) 1-17.
[9] X. Fan, W. Peng, Y. Li, X. Li, S. Wang, G. Zhang, F. Zhang, Advanced Materials, 20 (2008) 4490-4493.
[10] X. Meng, D. Geng, J. Liu, M.N. Banis, Y. Zhang, R. Li, X. Sun, The Journal of Physical Chemistry C, 114 (2010) 18330-18337.
[11] H. Chen, D. Shao, J. Li, X. Wang, Chemical Engineering Journal, 254 (2014) 623-634.
[12] P. Nuengmatcha, R. Mahachai, S. Chanthai, Oriental journal of chemistry, 30 (2014) 1463-1474.
[13] P.L. Meena, A.K. Surela, J.K. Saini, L.K. Chhachhia, Environmental Science and Pollution Research, 29 (2022) 79253-79271.
[14] J. Yang, T. Xie, C. Liu, L. Xu, Materials, 11 (2018) 1359.
[15] S.A. Hashemi, S.M. Mousavi, R. Faghihi, M. Arjmand, S. Sina, A.M. Amani, Radiation Physics and Chemistry, 146 (2018) 77-85.
[16] S. Bashiri, B. Ghobadian, M.D. Soufi, S. Gorjian, Materials Science for Energy Technologies, 4 (2021) 119-127.
[17] S. Prabhu, S. Bubbly, S. Gudennavar, Advanced Composite Materials, 32 (2023) 602-628.
[18] G.F. Knoll, Radiation detection and measurement, John Wiley & Sons, 2010.